WRF-Chem Intro - *High Performance Simulation*
Computational Mathematics and Data Analytics 2021-2022

Lorena Pérez Gálvez 1535868

Artur Llabrés Brustenga 1528792

Xabier Oyanguren Asua 1456628

1 Dust Simulation

Following the practice guide, we simulate the time evolution of the dust employing three different simulation options: `dust_opt=1`, `dust_opt=3` and `dust_opt=4`. We do so from 16 July 2010 00:00 to 19 July 2010 00:00, for which 4 equi-spaced frames are shown in figures 1, 2, 3 respectively.

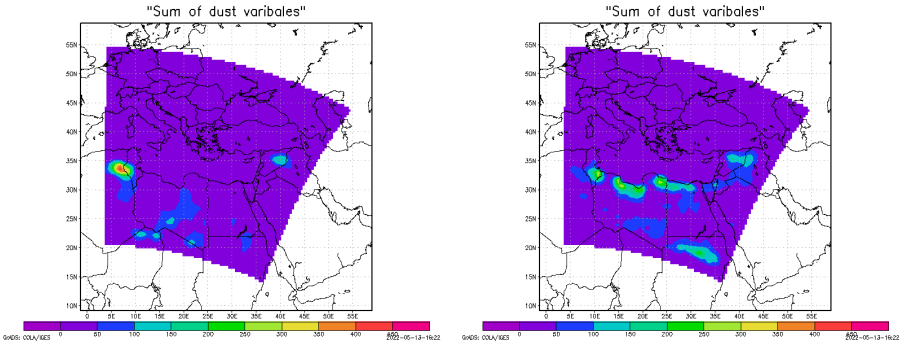

(a) 16/07 6h **(b)** 16/07 18h

(c) 17/07 6h **(d)** 17/07 18h

Figure 1: Plot of the predicted dust propagation from 16 July 2010 00:00 to 19 July 2010 00:00 (4 different equi-spaced frames in that interval). Employing dust simulation option 1 of WRF_Chem, following the practice guide.

To begin with, the dust simulation option 2 does not show any significant amount of dust in the simulated interval, as the colorbar range shows. Options 1 and 4 on the other hand, do predict some dust will appear, but only in Africa and the Arabian peninsula, which is to be expected for the simulated region at a random day (due to their closeness or inclusion in the Sahara desert).

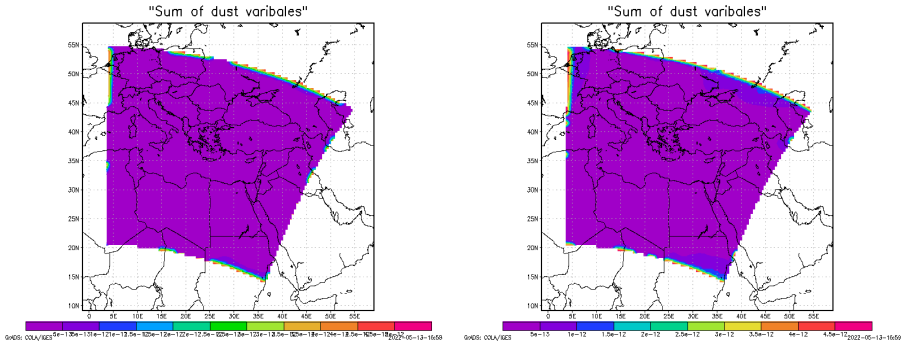

(a) 16/07 6h **(b)** 16/07 18h

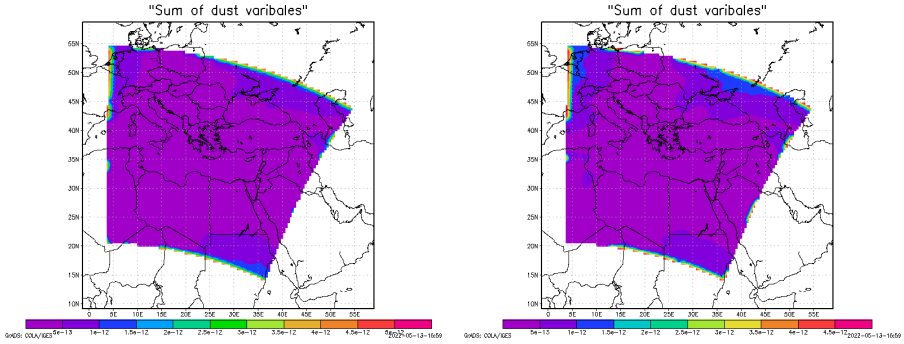

(c) 17/07 6h **(d)** Zoom-in Dom.2

Figure 2: Plot of the predicted dust propagation from 16 July 2010 00:00 to 19 July 2010 00:00 (4 different equi-spaced frames in that interval). Employing dust simulation option 3 of WRF_Chem, following the practice guide.

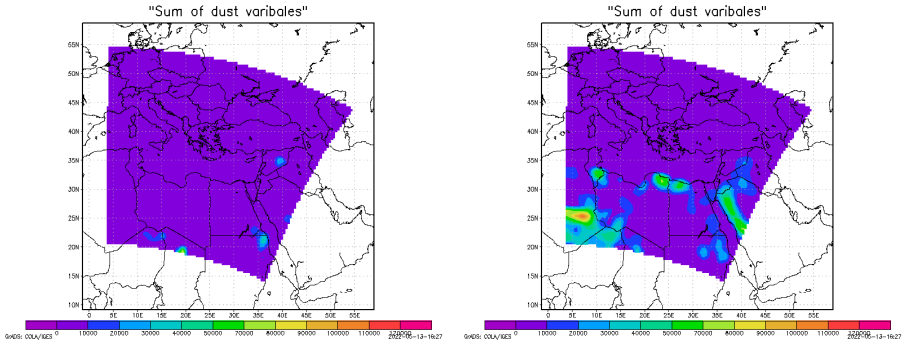

(a) 16/07 6h **(b)** 16/07 18h

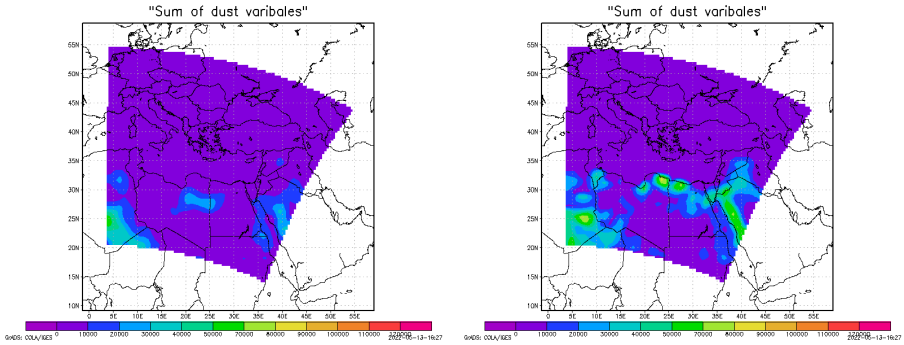

(c) 17/07 6h **(d)** 17/07 18h

Figure 3: Plot of the predicted dust propagation from 16 July 2010 00:00 to 19 July 2010 00:00 (4 different equi-spaced frames in that interval). Employing dust simulation option 4 of WRF_Chem, following the practice guide.

2 Postprocessing

Given the WRF-Chem output files provided in the practice guide, we run the ARW post-procesing tool as done in the previous section and the previous exercises to generate an adequate `.ctl` file. In order to analyse the variables within it, we employ a Python script where the library `netCDF4` is employed to open the `.ctl` file. Following, the practice guide we then choose a meteorological station, the one in Montcada i Reixac, for which we look for the closest latitude and longitude in the simulated grid. Over this point, we check how different state variables like the temperature 2 m above the surface or the wind speed and direction vary throughout the day. These are plotted in Figure 4. We also look at the predictions for some contaminant variables like the particles smaller than 10 microns `PM10` or the ozone O_3 and nitrogen dioxide NO_2 concentrations, shown in Figure 5. We do so, because for this station we also have the empirical observations made on that day (data that can be found in https://analisi.transparenciacatalunya.cat/Medi-Ambient/Qualitat-de-l-aire-als-punts-de-mesurament-autom-t/tasf-thgu/data). We plot these empirical contaminant variables in Figure 6.

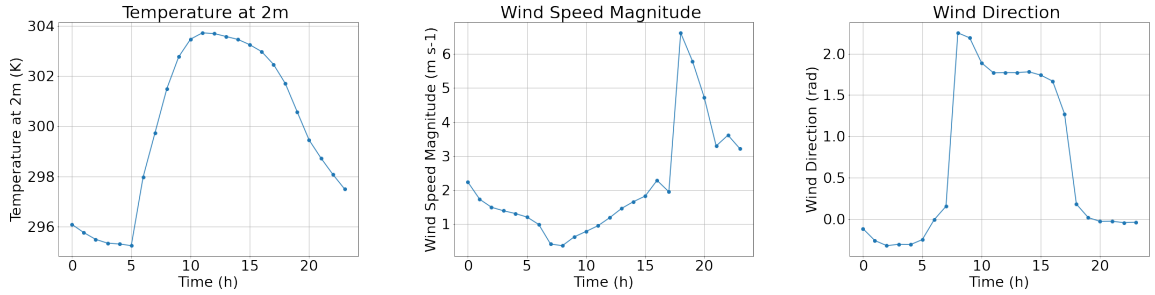

(a) Temperature at 2 meters **(b)** Wind speed magnitude **(c)** Wind angle

Figure 4: Plots of the simulated temperature 2m over the surface and wind speed and angle predicted over the meteorological station of Montcada i Reixac, from 20 July 2015 00:00 to 20 July 2015 23:00.

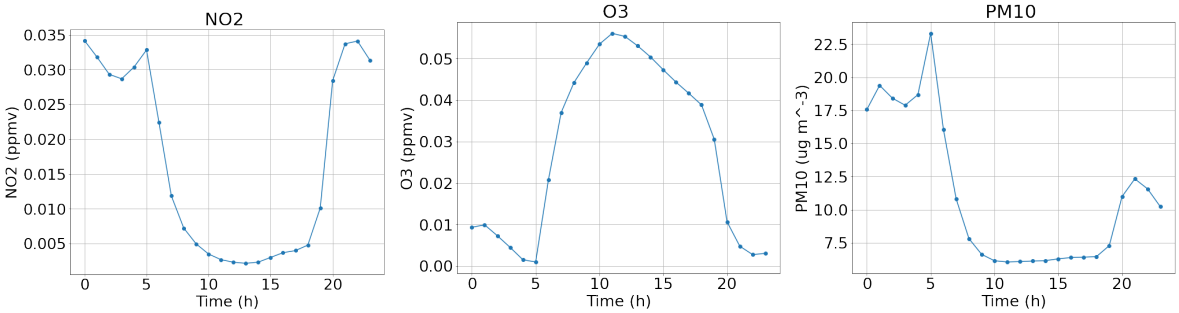

(a) NO_2 at surface level **(b)** O_3 at surface level **(c)** $10\mu m$ particles surface level

Figure 5: Plots of the experimental concentrations of NO_2, O_3 and particles smaller than 10 microns (PM10) observed in the meteorological station of Montcada i Reixac, from 20 July 2015 00:00 to 20 July 2015 23:00.

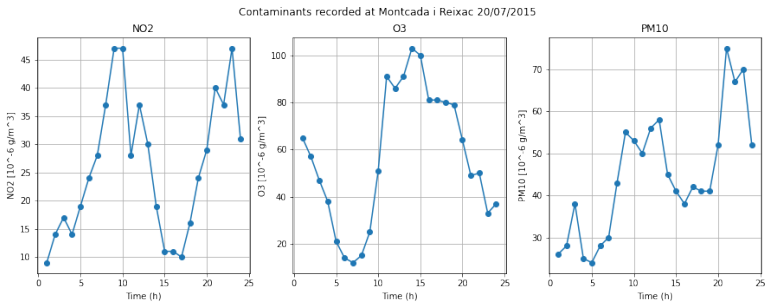

Figure 6: Plots of the experimental concentrations of NO_2, O_3 and particles smaller than 10 microns (PM10) predicted over the meteorological station of Montcada i Reixac, from 20 July 2015 00:00 to 20 July 2015 23:00.

We can see that even if the simulation results are not very accurate predictors when comparing Figures 5 and 6, the trends and shapes seem to be right. For instance, both in the simulated and the empirical data, the NO_2 concentration has two maximum regions, early in the morning and latter in the afternoon, while it gets an order of magnitude decreased by the evening. This is expectable, since NO_2 is a contaminant tightly related with the vehicle pollution and the greatest vehicle density in the highways occurs in the early morning and the afternoon, when humans go to- or get out of- work.

When it comes to the O_3 as well, the simulated trend matches the empirical one. There is a steep increase right after the morning NO_2 increase, which only gets back down when the second peak of NO_2 in the afternoon occurs. This could seem to be strange at first, since the rise in NO_2 appears to produce oppose effects. Yet, if one also observes the curve for the temperature, it turns out to perfectly match the ozone one. Thus, both a higher temperature and nitrogen oxide presence seem to be a requirement for higher O_3 concentration. Such a rise of tropospheric O_3 during the day and decay during the evening concurs indeed with our understanding of the theoretical mechanism of O_3 production, which is given by chemical reactions between oxides of nitrogen (NO_x) and volatile organic compounds (VOC) in the presence of heat and sunlight (correlated with the temperature).

Finally, when it comes to the particle concentration (for particles of sizes in the order of 10 microns), the predicted and empirical results only seem to have a matching trend towards the end of the afternoon, when a peak appears. Otherwise, they seem quite contrary, as do their magnitudes.

3 Study Case

In this exercise, we will plot and compare the simulation prediction and the gathered experimental data of the pollutant concentrations, both in Vic and Paradines. It must be said that this time we only know empirical information about O_3. However, we have likewise simulated NO_2 and $PM10$ data. We can see in Figures 8 and 10 the simulation predictions for the pollutants over Vic and Pardines, in Figure 11 their associated empirical data, while in Figures 7 and 9, we plot the simulated state variables analysed in the previous exercise for Vic and Pardines, respectiveley.

Once again, although the exact numbers do not precisely match, we see again that the trends are equal for the simulated or the empirical data. The concentration of O_3 increases notably in the early morning and only decreases back in the afternoon, in both locations.

The rationale and mechanism for all the variables seem to follow the same ideas explained in the previous exercise. The only exception perhaps is that in this case the 10 micron particle concentration seems to follow an increasing trend, with a lower concentration in the morning and maximum in the afternoon, just as the empirical data for Montcada did. Yet, we have no empirical data for Vic and Pardines to confirm its correctness.

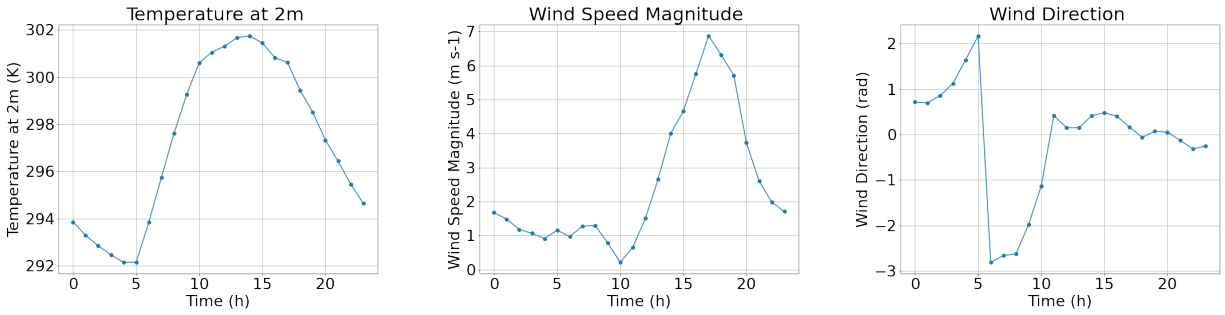

(a) Temperature at 2 meters **(b)** Wind speed magnitude **(c)** Wind angle

Figure 7: Plots of the simulated temperature 2m over the surface and wind speed and angle predicted over the meteorological station of Vic, from 20 July 2015 00:00 to 20 July 2015 23:00.

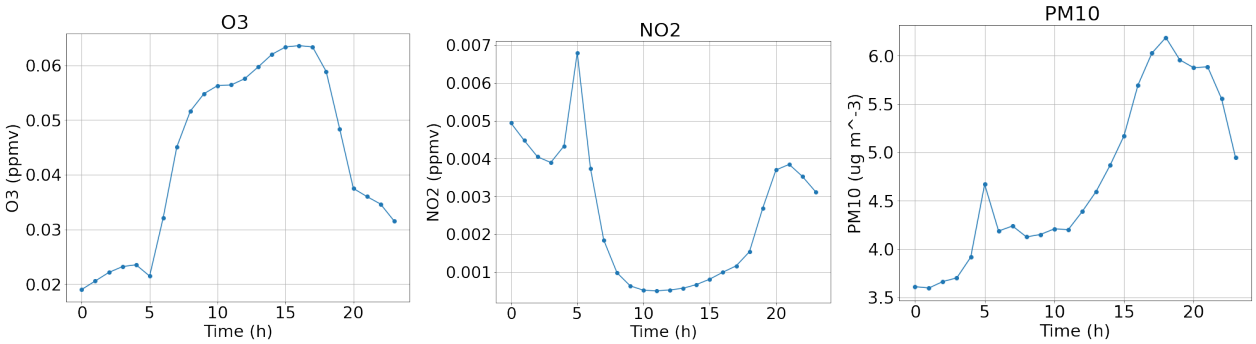

(a) O_3 at surface level **(b)** NO_2 at surface level **(c)** $10\mu m$ particles surface level

Figure 8: Plots of the simulated concentrations of NO_2, O_3 and particles smaller than 10 microns (PM10) predicted over the meteorological station of Vic, from 20 July 2015 00:00 to 20 July 2015 23:00.

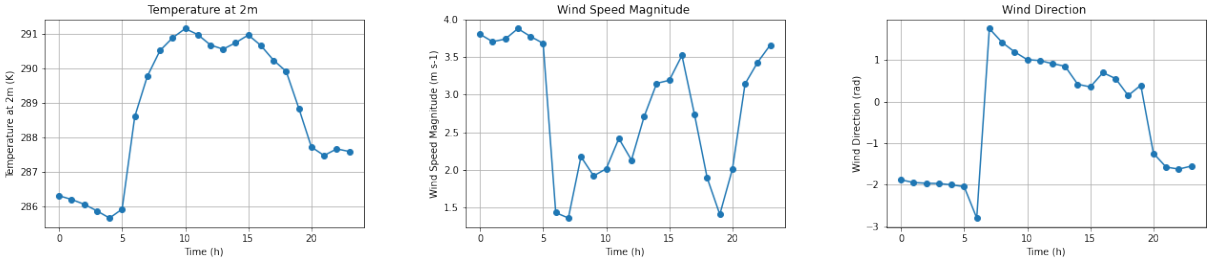

(a) Temperature at 2 meters **(b)** Wind speed magnitude **(c)** Wind angle

Figure 9: Plots of the simulated temperature 2m over the surface and wind speed and angle predicted over the meteorological station of Pardines, from 20 July 2015 00:00 to 20 July 2015 23:00.

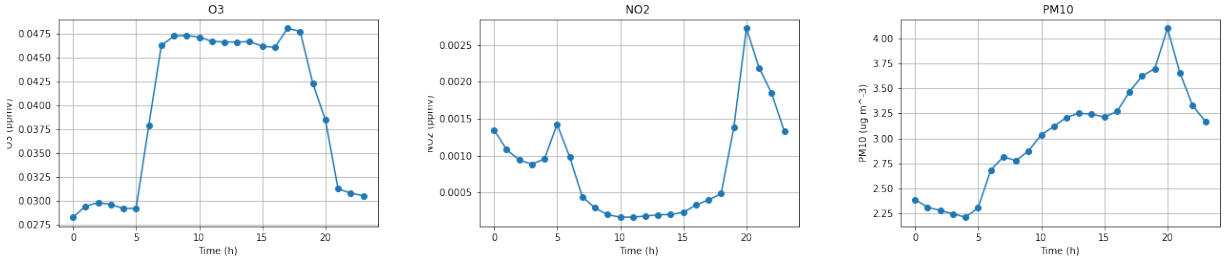

(a) O_3 at surface level **(b)** NO_2 at surface level **(c)** $10\mu m$ particles surface level

Figure 10: Plots of the simulated concentrations of NO_2, O_3 and particles smaller than 10 microns (PM10) predicted over the meteorological station of Pardines, from 20 July 2015 00:00 to 20 July 2015 23:00.

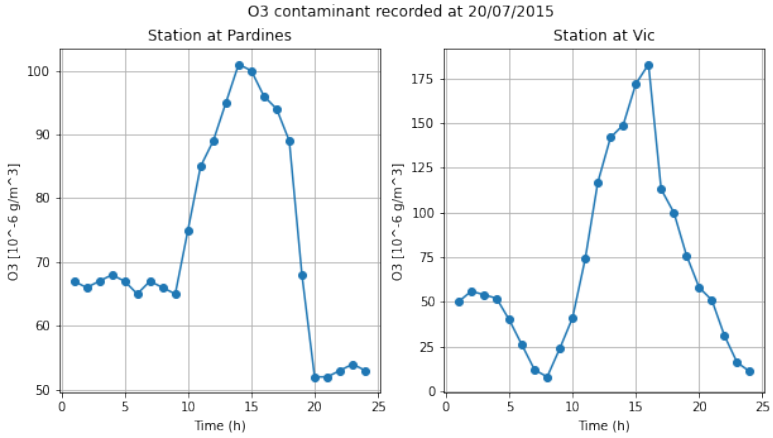

Figure 11: Plots of the experimental O_3 concentration observed in the meteorological stations of Vic and Paradines, from 20 July 2015 00:00 to 20 July 2015 23:00.